Unsaturated nanoporomechanics

Hoang Nguyen[a], Saeed Rahimi-Aghdam[b], and Zdeněk P. Bažant[c,1]

[a]Theoretical and Applied Mechanics Program, Northwestern University, Evanston, IL 60208; [b]Department of Civil and Environmental Engineering, Northwestern University, Evanston, IL 60208; and [c]Department of Civil and Environmental Engineering, McCormick School of Engineering, Northwestern University, Evanston, IL 60208

Contributed by Zdeněk P. Bažant, December 17, 2019 (sent for review November 5, 2019; reviewed by Paulo J. M. Monteiro and Franz-Josef Ulm)

Although some important advances in the modeling of sorption and hygrothermal deformations of nanoporous materials such as hydrated cement paste, shale, coal, and some other rocks and soils have already been made, a comprehensive nanoporomechanics theory remains elusive. Here we strive to formulate it based on Gibb's free energy of the solid–fluid system and on the recently derived Nguyen–Rahimi–Bažant (NRB) isotherm, which corrects the Brunauer–Emmett–Teller (BET) isotherm for the effect of hindered adsorbed water in filled nanopores and extends through the capillary range up to saturation. The challenge is to capture all of the basic types of relevant published experimental data, including 1) a complete sorption isotherm of hydrated cement paste (including the capillary range), 2) pore size distribution, 3) autogenous shrinkage, 4) drying shrinkage and swelling, 5) water loss or humidity change due to heating, 6) thermal expansion at various humidities, and 7) water loss of specimens caused by compression. The previous models can fit only a few data types. The present model fits all of them. It is ready for computer simulations needed to minimize the deleterious moisture effects on long-time deformations, cracking damage, and fracture in concrete infrastructure and thereby to reduce indirectly the enormous carbon footprint of concrete. Adaptations to shale, coal beds, etc., are possible.

unsaturated poromechanics | hindered adsorbed water | Biot coefficient | shrinkage | swelling

Poromechanics of liquid-saturated materials is by now a classical subject (1), in essence formulated by Biot (2) in the 1940s. Poromechanics of unsaturated materials with menisci separating liquid and vapor phases is a recent creation, with Coussy (3, 4) as the main contributor. However, major knowledge gaps remain and no predictive mathematical model exists. It is needed to tackle the shrinkage, creep, durability, fracturing, freezing, and degradation of hydrated cement paste and concrete, phenomena that shorten the lifetimes of infrastructure [and thus indirectly enhance worldwide CO_2 emissions in the long run (5, 6)]. These materials are strongly hydrophilic. Most water is adsorbed in nanopores of average width <1 nm and exerts, on nanopore walls, disjoining pressures of the order of 100 MPa. Because the capillary pores containing liquid water and vapor do not percolate, the surface diffusion of water along the nanopores is what controls water transport (see ref. 7 for microstructure details). Similar problems arise for gas or oil shale, coal beds, and other nanoporous materials. Here we develop a comprehensive mathematical model of unsaturated poromechanics based entirely on a recent mathematical derivation of the Nguyen–Rahimi–Bažant (NRB) sorption isotherm (8) (for posting of the original idea, see ref. 9, ArXiv:1812.11235).

NRB Isotherm for Nanomacropore Filling

Strongly hydrophilic nanoporous materials, such as hydrated cement paste or several compositions in shale, Vycor glass, and cellulose, exhibit multimolecular adsorption, for which the BET isotherm (10) has normally been used. Unfortunately, though, the BET does not work for nano- and microporous materials, such as hydrated cement paste, in which the average nanopore width is <1 nm. The problem is that BET theory does not consider the hindered adsorbed water, consisting of adsorbed water layers that completely fill the pores. Another old theory, BJH (11), relating sorption to pore size distribution, uses a relation of a unique meniscus curvature to h but, unlike BET or NRB, is not based on statistical expectations of the rates of evaporation and condensation of molecules.

These limitations have recently been overcome by the NRB theory of Nguyen, Rahimi, and Bažant (8), which was derived by statistics of water adsorption, condensation, and evaporation similar to BET (10) but with the crucial difference that, due to gradual filling of nanopores, the surface area exposed to vapor decreases with the number n of adsorbed molecular layers and depends on pore size distribution. This decrease is described by a surface area reduction factor β_n. Its realistic choice is a self-similar function, i.e., a power function, which leads to the NRB isotherm $\theta(h)$,

$$\beta_n = 1 \text{ for } n = 0;\ \beta_n = n^{-q} \text{ for } n = 1, 2, 3, \ldots \quad [1]$$

$$\theta = \frac{\Gamma_a}{\Gamma_1} = \frac{\sum_{n=1}^{\infty} \beta_n n h^n}{c_T^{-1} + \sum_{n=1}^{\infty} \beta_n h^n} = \frac{\mathrm{Li}_{q-1}(h)}{c_T^{-1} + \mathrm{Li}_q(h)}, \quad [2]$$

where h is relative vapor pressure (or humidity), $h = p_v/p_{sat}(T)$; p_v is vapor pressure in the pores, $p_{sat}(T) = p_v$ at saturation at absolute temperature T; Γ_a is mass of adsorption layer (including both free and hindered adsorbed layers, as defined in refs. 12 and 13); Γ_1 is mass of full monomolecular layer; $c_T = c_0 e^{Q_l/\bar{R}T}$; Q_l is heat of liquefaction of water; q, c_0 are empirical parameters; and $\mathrm{Li}_q(h) = \sum_{n=1}^{\infty} h^n/n^q$ is Jonquière function (or polylogarithm). The alternative $\beta_n = (1+n)^{-q}$, $n = 0, 1, 2, \ldots$ (8) fits the data almost as well but gives a lower initial isotherm slope than the BET, which is unrealistic since the exposed area is not being reduced during the first layer filling. Also note that we do not address here the isotherm hysteresis.

Significance

The hygrothermal effects play a major role in cracking, degradation, and durability of concrete infrastructure and indirectly in structural safety under overloads such as earthquake. Besides costs, the consequences are premature replacements of bridges, pavements, etc., which, in the long run, increase the demand for cement production, whose CO_2 emissions already rival those of all of the cars and trucks in the world and, following the current trend, would exceed them greatly. Our theory will help to lengthen lifetimes and enhance safety. It can also be adapted to shale, coal beds, and other nanoporous materials.

Author contributions: Z.P.B. conceived the NRB isotherm; H.N., S.R.-A., and Z.P.B. conceived research, performed research, and wrote the paper; and H.N. and S.R.-A. analyzed data.

Reviewers: P.J.M.M., University of California, Berkeley; and F.-J.U., Massachusetts Institute of Technology.

The authors declare no competing interest.

[1]To whom correspondence may be addressed. Email: z-bazant@northwestern.edu.

First published January 31, 2020.

Eq. **2** was used in ref. 8 to fit the sorption isotherm tests of hydrated cement paste and concrete. Although much better than BET, it still did not represent well the capillary range, $h > 0.9$, and incorrectly tended to ∞ as $h \to 1$. The cause, revealed by looking at the statistical derivation of the NRB isotherm in ref. 8, equations 16 and 25, is that the series summation unrealistically implies further condensed water layers (many more than five) to be added on top of the initial ones, despite virtually no interaction with the solid adsorbent. Instead, lateral interactions between water molecules become more important, as in liquid (capillary) water. This can generally be handled by adjusting function β_n for high n (while ensuring convergence of the sums in [**2**]). For hydrated cement paste, this appears unimportant, but is needed for Vycor, coal, and other nano-micro-porous materials with higher capillary porosity.

To relate β and pore size distribution, we set (ref. 8, equations 51 and 52)

$$F_w = 1 - \beta(w), \quad f_w = -\mathrm{d}\beta(w)/\mathrm{d}w, \qquad [3]$$

where $\beta(w)$ is a continuous version of β_n, $w = 2n\delta_1$ is continuous variation of pore width, and δ_1 is thickness of the full adsorbed monolayer; $F(w)$ is cumulative density function (cdf) or pore size (or width) w, and $f(w)$ is probability density function (pdf) of w. $F(w)$ has been described by an exponential (14) or a power law (14, 15), but only the latter, being self-similar, can work over a broad size range.

The geometric characteristics of the pores per unit volume of porous material are best defined in parametric form, in terms of h. The pore width can be inferred from the humidity level, h_f, at which the pore gets filled. Let $V_f(h)$ be volume of pores filled at h by adsorbed water and $A_f(h)$ be the portion of surface area of pores completely filled by condensed water (which means that the $1 - A_f(h)$ is the portion of surface area exposed to vapor at h). Also note that $V_f = \int w \mathrm{d}A_f$ or $\mathrm{d}V_f = w\mathrm{d}A_f$, where w is pore width, and that, according to Fig. 1*B*, $\mathrm{d}A_f = -A_0\,\mathrm{d}\beta$ and $\mathrm{d}V_f = -A_0(w/2)\,\mathrm{d}\beta$, where A_0 is surface area of dry pores (at h = 0). Consequently,

$$w_f(h) = \frac{\mathrm{d}V_f(h)\,/\,\mathrm{d}h_f(h)}{\mathrm{d}A_f(h)\,/\,\mathrm{d}h_f(h)} = H[h_f(h)] \qquad [4]$$

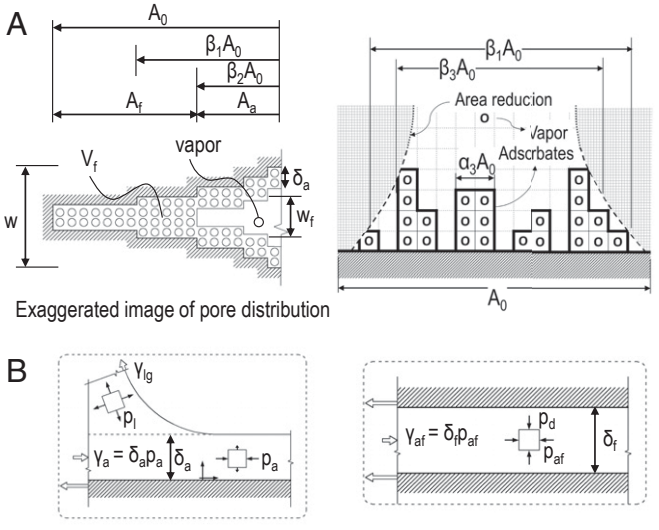

Fig. 1. (*A*) Adsorption of new molecular layers reduces surface area exposed to vapor. (*B*) Stress states of different water phases where meniscus meets adsorbent wall.

$$A_f(h_f) = -A_0 \int_0^{h_f} \frac{\mathrm{d}\beta}{\mathrm{d}h}\,\mathrm{d}h = -A_0 \int_0^{w_f} \frac{\mathrm{d}\beta}{\mathrm{d}w}\,\mathrm{d}w \qquad [5]$$

$$V_f(h_f) = -\frac{A_0}{2}\int_0^{h_f} w(h)\frac{\mathrm{d}\beta}{\mathrm{d}h}\,\mathrm{d}h = -\frac{A_0}{2}\int_0^{w_f} w\frac{\mathrm{d}\beta}{\mathrm{d}w}\,\mathrm{d}w \qquad [6]$$

$$\beta(h_f) = -\frac{2}{A_0}\int_0^{h_f} \frac{1}{w(h)}\,\frac{\mathrm{d}V_f(h)}{\mathrm{d}h}\,\mathrm{d}h \ \text{(as inverse)}, \qquad [7]$$

where w_f is maximum width of pores filled by adsorbed water at the filling humidity $h = h_f$, and functions $w_f(h)$ and $V_f(h)$ define parametrically the cumulative pore size distribution of w_f as a function of V_f (previously studied in refs. 15 and 16). Here we assume that the free adsorbed layers on the opposite faces keep uniform thickness δ_a up to the point where $2\delta_a = w_f$ (Fig. 1*B*), which is a simplification. In reality, a segment of a somewhat wider pore near this point is also filled by adsorbed water, which we neglect (12, 17). Inverting [**4**], one gets humidity h_f at which a pore of given width w_f gets filled:

$$h_f = H^{-1}(w_f). \qquad [8]$$

Thermodynamics of Pore Water and Poroelastic Constitutive Relations

The chemical potential μ, i.e., Gibbs free energy per unit mass of pore water, is generally defined by $\mathrm{d}\mu = \mathrm{d}p_V/\rho_a$, where p_V is hydrostatic pressure in any phase of water. In free adsorption, the stress state is close to biaxial, and so $p_V = 2p_a/3$, where $p_a = -\gamma_a/\delta_a$, where $-\gamma_a$ is spreading pressure in the free adsorbed layer (γ_a is surface tension). Expressing $\mathrm{d}\mu = \mathrm{d}p_V/\rho_a = \mathrm{d}(2p_a/3\rho_a)$ in terms of h yields

$$\mathrm{d}p_a(h) = -\mathrm{d}\gamma_a(h)/\delta_a(h) = -\rho_a(\bar{R}T/M_w)\mathrm{d}(\ln\,h). \qquad [9]$$

For hindered adsorption in filled pores, $p_V = (2p_{af} + p_d)/3$, where p_d is disjoining pressure, acting on pore walls, and p_{af} is spreading pressure in hindered adsorbed layer. For a specific pore width w, filled at a specific h_f, we get (12, 13)

$$p_d(h) = \kappa\rho_a(\bar{R}T/M_w)\ln(h/h_f) \quad \text{for} \quad h \geq h_f, \qquad [10]$$

where $\kappa = 3/(1 + 2p_a/p_d)$ (its value will need to be estimated by atomistic simulations). The mass density, ρ_a, of adsorbed water is considered as approximately constant and probably $\rho_a \approx$ mass density of ice = 91% of mass density ρ_l of liquid water or even smaller due to the steric effect caused by the large side group on the surface of hydrates.

The equivalent pore pressure, π, in a porous material must be defined by work. We may imagine an expansion, $\mathrm{d}\varphi$, of the pore volume per unit volume of material, and the $\mathrm{d}\Phi = \pi\,\mathrm{d}\varphi$ is the corresponding Helmholtz free-energy increment (φ is porosity). Poromechanics based on Helmholtz free energy were used by Coussy (3, 4, 18), but in ref. 19 it was shown that using the Gibbs free energy is more convenient to compute π. Ψ is a complementary potential, for which $\mathrm{d}\Psi = \varphi\mathrm{d}\pi$. Including volumetric stress σ and strain ϵ, we define the equivalent pore pressure by the Gibbs free-energy increment:

$$\mathrm{d}\Psi = \epsilon\mathrm{d}\sigma + \varphi\mathrm{d}\pi. \qquad [11]$$

To formulate the constitutive equation, all of the phases of water are considered to be locally (in a macrocontinuum point) in thermodynamic equilibrium. This requires the chemical potential, μ, to be the same in all pore water phases. According to the Kelvin and Laplace equations and the ideal gas equation for water vapor (12, 13), we have

$$\mu = (\bar{R}T/M_w)\ln\,h, \qquad [12]$$

where $\bar{R}$ is the gas constant (8.314 $\mathrm{J{\cdot}K^{-1}{\cdot}mol^{-1}}$), and M_w is molecular weight of water (18.02 g/mol). The sum of the chemical potential increments of masses m_i of all water phases

gives the extensive potential—the Gibbs free energy, Ψ_w, of all fluid phases. Its increment, therefore, is $\mathrm{d}\Psi_w(h)=\sum_i m_i \mathrm{d}\mu = \varphi\,\mathrm{d}\pi(h)$, which is the Gibbs–Duhem equation; m_i $(i=1,2,..)$ are the masses of fluid phases. So,

$$\begin{aligned}\mathrm{d}\Psi_w(h) \;=\; & \varphi\,\mathrm{d}\pi(h)=\varphi S_v \mathrm{d}p_v(h)/\rho_v+\varphi S_l \mathrm{d}p_l(h)/\rho_l \\ & +\; A_a\delta_a \mathrm{d}[2p_a(h)/3\rho_a]+A_f\delta_f \mathrm{d}[2p_{af}(h)/3\rho_a] \\ & +\; \delta_f A_f \mathrm{d}[p_d(h)/3\rho_a]-\mathcal{S}_{en}\mathrm{d}T, \end{aligned} \qquad [13]$$

where $A_a=A_0-A_f=A_0\beta$, $\delta_f=V_f/A_f$ is an equivalent thickness of the filled volume, $\mathcal{S}_{en}=\sum_i \mathcal{S}_{en,i}$ is the sum of the entropies of all water phases; S_l, S_v are saturation degrees of liquid and vapor equaling their volumes as fractions of pore space volume φ, and p_l, p_v are their pressures (capillary pressure $p_c=p_v-p_l\approx -p_l$); and $\mathrm{d}\gamma_a=-\delta_a \mathrm{d}p_a$ is surface tension. From Eq. **2**, the liquid, or capillary, portion $S_l=V_l/V_p$ of the total pore volume is

$$V_l=\theta(q,h,T)A_0\delta_1-\theta(\bar{q},h,T)A_0\delta_1 \quad (\bar{q}>q). \qquad [14]$$

Here we subtract the volume of the adsorbed water layers, whose thickness (characterized by $\bar{q}$) may be identified from adsorption tests of hydrated cement paste and extrapolation of the linear portion of the curve of adsorbed volume vs. thickness. This yields (20) the maximum adsorption thickness of 4.54 molecular layers.

By integration of h at constant T, we get

$$\begin{aligned}\pi(h) \;=\; & \frac{\bar{R}T\rho_l}{M_w}\int_0^h \mathrm{d}[S_l(h)\ln h]+\kappa_a\frac{\bar{R}T\rho_l}{M_w}\int_0^h \Gamma_a(h)\mathrm{d}(\ln h) \\ & +\; \frac{1}{A_0}\int_0^{h_f}\int_{h_f}^{h}\mathrm{d}[p_d(h)]\mathrm{d}[A_f(h_f)]. \end{aligned} \qquad [15]$$

Despite the difference in the spreading pressures (the second term) in the free adsorbed water, which is in direct contact with vapor, and in the hindered adsorbed water (Fig. 1*B*), which is not, we need to consider only the pressure resultant $-\gamma_a$ (=−surface tension) over thickness δ_a which acts along the total surface area $A_0=A_a+A_f$ and is modified by κ_a in the hindered layers. Prefactor κ_a in Eq. **15** also ensures the work of hydrostatic pressure on a volume to be equal to the work of the pressure resultant on an area.

The last, disjoining, term of Eq. **15**, unlike the other two, includes both humidity integral and area integrals. This term may be approximated as $\kappa_d\lambda(h)(\bar{R}T\rho_a/M_w)\ln(h/h_{f0})$, where $\lambda(h)=A_f(h)/A_0$ is the area fraction experiencing disjoining pressure; h_{f0} characterizes the smallest pore width that can be filled by water (and thus has the maximum disjoining pressure); for calcium silicate hydrate (C-S-H), the main binding phase in the hydrated cement paste in which most of the adsorbed water resides, the average nanopore width is <1 nm [which occurs at $h_{f0}\approx 1\%$ (17)]; κ_d is an empirical factor taking into account 1) the prefactor $1/A_0$ in Eq. **15**, 2) the reduction ratio due to the roughness of opposite surfaces, limiting the proximity of walls and hence the disjoining pressure p_d (7), and 3) κ in Eq. **10**. In Eq. **15**, even though the first term is always negative and asymptotically equal to zero at both $h=1$ and 0, the second and third terms are not. The pressure, p_d, increases with h up to saturation [this is one cause of microstructure prestress buildup in hydrated cement (13)]. The pressure p_d in a nanopore, exerted locally on A_f, contributes not only to the shrinkage/swelling of the pores but also to the creep deformation. Indeed, it triggers a slip between adjacent sheets that are inclined with respect to the wall under disjoining pressure. This observation has been formulated and validated by the microprestress-solidification theory (21, 22). Therefore, a higher humidity leads to change both in microprestress and in apparent viscosity in the water interlayer (23).

The poroelastic volumetric part of the constitutive relation of unsaturated porous elastic solid follows from the first variation of Ψ, as in ref. 19, equations 16 and 17:

$$\mathrm{d}\epsilon-\alpha\,\mathrm{d}T \;=\; \frac{1}{K}\mathrm{d}\sigma+\frac{b}{K}\mathrm{d}\pi \qquad \left(\frac{b}{K}=\frac{1}{H}\right) \qquad [16]$$

$$\mathrm{d}\zeta-\alpha'\mathrm{d}T \;=\; \frac{c}{R}\mathrm{d}\sigma+\frac{1}{R}\mathrm{d}\pi \qquad \left(\frac{c}{R}=\frac{1}{H}\right). \qquad [17]$$

Here σ is volumetric stress acting on the solid phase (positive for tension, while π is positive for compression); ζ is divergence of the displacement vector of all of the pore water (measurable when drained); K, R are bulk elastic moduli of the solid and fluid phases, and H is the solid–fluid cross-modulus; and α, α' are thermal expansion coefficients of the porous medium and of the pores. The compliances (ref. 19, equations 11–24) are

$$\frac{1}{K}=\frac{\partial^2\Psi}{\partial\sigma^2},\ \frac{1}{R}=\frac{\partial^2\Psi}{\partial\pi^2},\ \frac{1}{H}=\frac{\partial^2\Psi}{\partial\sigma\,\partial\pi}. \qquad [18]$$

The Biot coefficient, the Skempton coefficient, and the inverse of the Biot modulus are

$$\begin{aligned} & b=-\left.\frac{\partial\sigma}{\partial\pi}\right|_{\epsilon=0}=\frac{K}{H},\ c=-\left.\frac{\partial\pi}{\partial\sigma}\right|_{\zeta=0}=\frac{R}{H}, \\ & \frac{1}{M}=\left.\frac{\partial\zeta}{\partial\pi}\right|_{\epsilon=0}=\frac{1}{R}-\frac{K}{H^2}. \end{aligned} \qquad [19]$$

Autogenenous Shrinkage and Swelling

To study the long-term behavior, the calculation of deformation due to fluid pressure must be combined with the hydration reaction model. The main long-term deformations are the autogenous (chemically induced) shrinkage and the swelling. It was widely believed that the hydration process ceases after about 1 y. But that could be true only for specimens thin enough to dry to a uniform humidity $h<0.5$ within such time. In the core region of a thick wall in a drying environment, a high humidity may last for decades, even centuries (19). The main cause of such long-lived hydration and its decaying rate is that, after the first day, the remaining anhydrous cement grains get enveloped by gradually thickening cement hydrate shells of extremely low permeability, and the water transport toward the anhydrous grain gets slower as these shells thicken. The thickening further causes a decrease of the pore relative humidity, h, as well as the chemical potential of water, causing the slowdown of hydration. This was experimentally demonstrated by refs. 24–26 and mathematically described by ref. 27.

Autogenous shrinkage has been shown (19) to be caused by self-desiccation, which is, according to RILEM TC 196-ICC (28), defined as the reduction of the relative humidity, h, in a sealed system (no external drying). The cause of self-desiccation is the hydration reaction. The relative humidity decrease due to hydration depends significantly on water-to-cement ratio w/c. As w/c decreases, self-desiccation increases and so does autogenous shrinkage. These are long-lived decaying phenomena, continuing for decades with no bound. The autogenous shrinkage might be augmented and prolonged by creep due to disjoining pressure. When immersed in water, water diffuses in and the specimen swells, as affirmed by many data. For the diffusion, the model developed in ref. 29 is used. The swelling is also a long-lived, multidecade, phenomenon and advances roughly logarithmically

(30). In refs. 19 and 31 it was shown that the cause of swelling is the expansiveness of the hydration reaction, possibly augmented by creep due to disjoining pressure of hindered adsorbed water in filled nanopores, which is also created by hydration as more and more calcium silicate hydrate (C-S-H) gets produced.

To determine the effect of nano- and microporosity on bulk modulus K in [**16**] and [**17**], we use the semiempirical equation for Young's modulus,

$$E = E_s(1-\varphi_0)^s; \quad K = E/3(1-2\nu), \qquad \textbf{[20]}$$

where ν (Poisson ratio, about 0.18 for concrete) and s depend on pore size distribution. Helmuth and Turk (32) showed that $s = 3$ for hydrated cement (Fig. 2*C*), and Kováčik (33) showed s = about 2 for porous glass and 1.14 to 1.64 for porous alumina. For the Young's modulus of the mixture of C-S-H and anhydrous phase, $E_s = 80$ GPa (32, 34).

For elastic deformation at constant π, $\mathrm{d}\epsilon = \mathrm{d}\sigma/K$, however, for long-time loading, the bulk compliance $1/K$ must be replaced by the bulk compliance function for creep, $1/J(t,t')$, where t, t' are the current time and age at loading (13). The deformation, therefore, takes into account the entire loading history.

Verification by Experimental Data

There exist seven different types of experiments that should be describable by a realistic nanoporomechanical model. Good fits of only some of these experiments, often only one, two, or rarely three, have been presented in many studies. However, such selective data can be fitted by many different models. Fitting all of them with one and the same model has been a challenge and is achieved here. Only such a comprehensive agreement with all of the types of experiments gives high (although not absolute) confidence that the model is correct and unique.

1. Sorption Isotherm. Simulations on hardened cement paste (HCP) were compared to test data from refs. 35 and 36. To be sure that hygroscopic equilibrium with nearly uniform h has been achieved within about 2 d, we choose only thin enough specimens, of minimum thickness ≈1 mm. Fig. 2 *A* and *B*, *Left* shows the data for two HCP specimens with different w/c. Satisfactory fits are evident. The fit parameters are $c_T = 5.19$, $q = 2.35$, $\bar{q} = 2.82$ for Fig. 2*A* and $c_T = 4.18$, $q = 2.18$, $\bar{q} = 2.61$ for Fig. 2*B*;

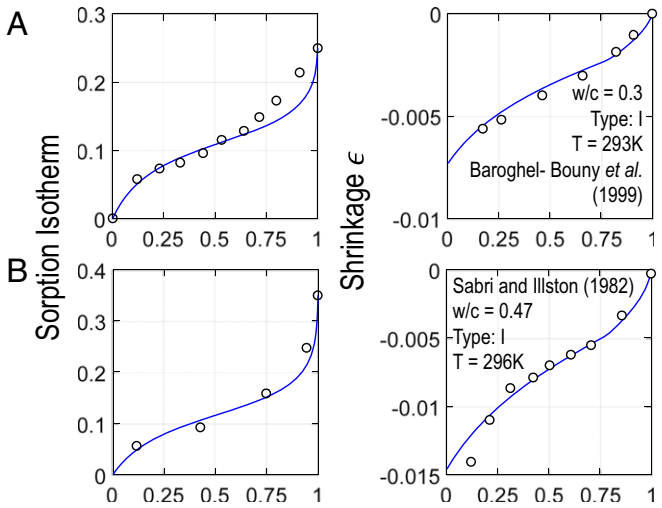

Fig. 2. Correspondence of sorption isotherm and drying shrinkage of hardened cement pastes. (*A* and *B*) Tests by (*A*) Baroghel-Bouny et al. (35) and (*B*) Sabri and Illston (36).

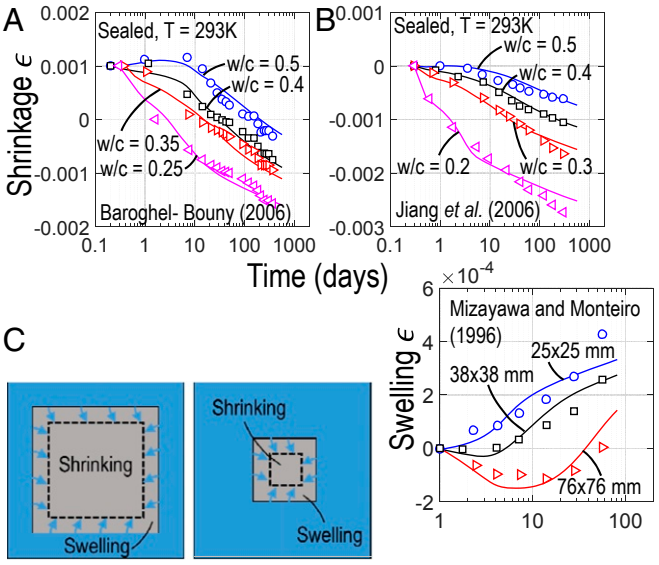

Fig. 3. (*A* and *B*) Measured (37, 38) and calculated autogenous shrinkage of concrete. (*C*) Measured (40) and calculated swelling simultaneous with autogenous shrinkage of concrete submerged in water.

φ_0 (0.24 for Fig. 2*A* and 0.35 for Fig. 2*B*) was estimated from its relation to w/c as in ref. 32.

2. Drying Shrinkage. The shrinkage behaviors of the same HCP samples as in *1. Sorption Isotherm* were fitted with the same model parameters. The geometrical parameters were $\kappa_a = 35.46 \cdot 10^8$, $\kappa_d = 0.08$ for Fig. 2*A* and $\kappa_a = 5.85 \cdot 10^8$, $\kappa_d = 0.08$ for Fig. 2*B* (data for $h < 0.05$, which took >40 d to equilibrate, were omitted from the fitting). Fig. 2 *A* and *B*, *Right* demonstrates a satisfactory fit. The correspondence of shrinkage with sorption isotherms supports and validates the present model. This model captures not only the behavior of water phases but also their effect on the solid skeleton, as indicated by Eq. **15**. From *1. Sorption Isotherm* and *2. Drying Shrinkage*, note that, for HCP, the adsorbed water makes at high h a greater contribution than the capillary water, due to a low value of V_l in [**15**] (its effect, though, peters out at low h). Note that creep and drying shrinkage were inseparable and total deformation was computed based on ref. 19.

3. Autogenous Shrinkage. We begin with Baroghel-Bouny et al.'s (37) tests of autogenous shrinkage of cement pastes at different w/c. Fig. 3*A* compares the calculated curves with the measured points. The default parameters of the hydration model giving the hydration degree were reported in ref. 27. They were used to calculate the self-desiccation and the evolutions of capillary and nanopore volumes and of material strength. At 1 y of hydration, the parameters approach the "hardened" values; $c_T = 4.69$, $q = 2.27$, $\bar{q} = 2.72$, $\kappa_a = 27.16 \cdot 10^8$, $\kappa_d = 0.08$, $\varphi_0 = 0.295$ for $w/c = 0.4$. Bulk modulus K is assumed to depend linearly on the hydration degree. As seen, the agreement is good, showing correctly the initial swelling in cement pastes with high w/c, even though the model was calibrated only by matching 1-mo K for $w/c = 0.4$. The rest is prediction.

Next, consider the tests of Jiang et al. (38), which are quite similar to Baroghel-Bouny et al.'s (37). The only significant difference is that the cement contained higher percentages of C_3A and of a high-range water reducer at low w/c ratios. Fig. 3*B* shows the predicted results agree well with the experiments. The autogenous shrinkage results are time dependent and the creep has a significant effect, as modeled by the update (22) of the

microprestress-solidification theory (13, 21). Note that the autogenous shrinkage curve has no horizontal asymptote (19) and the Biot coefficient is not constant but decreases as the elastic modulus increases due to hydration. The decrease has usually been neglected (39) but, as shown by Rahimi-Aghdam et al. (19), its effect is significant.

4. Swelling. Swelling of water-immersed specimens always occurs simultaneously with hydration and autogenous shrinkage. Recently, it was shown that the hydration process is always expansive (19, 31), even for decades, and that what drives all shrinkage, including autogenous, is pore humidity decrease. So, high pore humidity allows swelling to proceed unhindered by autogenous shrinkage, as documented by Mizayawa and Monteiro (40). They tested mortar prisms of different sizes, with $w/c = 0.3$, sealed at 1-d age, and then placed in a fog room. No previous model seems to fit these experiments. We use the same fitting parameters as in Fig. 2*A*. Fig. 3*C* compares the predicted versus experimental results for three different specimen sizes. Good agreement is seen. To model the drying, the nonlinear diffusion equation from ref. 29 is used. The creep due to disjoining pressures is included, too (19).

5. Hygrothermic Effect. We now focus on the temperature effect on the change of h per °K in small specimens with different w/c. The humidity change is observed to depend on the initial uniform humidity nonmonotonically, with no change at $h = 0$ and 1, as required; see in Fig. 4*A* the solid curve predicted using Eq. **2** with $c_T = c_{T0}\, e^{\Delta H_c/\bar{R}T}$ (Arrhenius law) and the derivative of the total water mass $m_w = \rho_l(T)\theta(q, h, T)A_0\delta_1$. The data in Fig. 4*A* are extracted from tests of HCP specimens cited in the legend. The fitting parameters are $q = 2.5$, $c_{T0} = 0.00361$, $\Delta H_c = 20{,}000$ J/mol, $\varphi_0 = 0.33$, corresponding to $w/c = 0.45$ (the effects of w/c ratio and cement type are embedded in β).

6. Thermal Dilatation. The temperature increase not only expands the porous solid skeleton, according to its thermal dilatation coefficient α, but also changes the fluid pressure acting on the pore walls (as a result of local humidity change mentioned in *5. Hygrothermic Effect*). This causes additional expansion.

The thermal dilatation coefficient, therefore, depends on h similarly to the hygrothermic coefficient. Fig. 4*B* shows a comparison with the test data cited in the legend. The same parameters as in 5. *Hygrothermic Effect* are used, along with $\kappa_a = 17.09 \cdot 10^8$, $\kappa_d = 0.08$, and the doubling of the dry-state

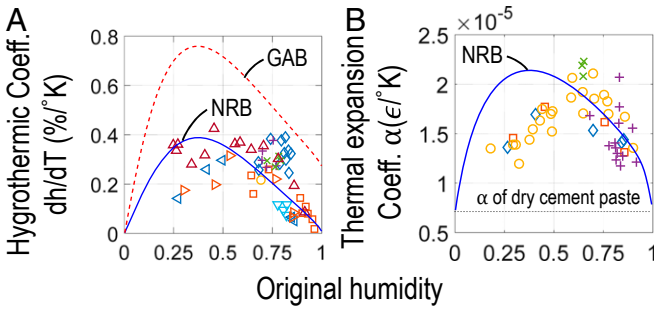

Fig. 4. (*A*) Hygrothermic coefficients corresponding to NRB theory and GAB theory, compared against tests of Nilsson (41), w/c = 0.4 (◇), w/c = 0.7 (□), w/c = 0.7 of silica (○); Persson (42), w/c = 0.37 (+), w/c = 0.48 (×), w/c = 0.75 (▽); Radjy et al. (43) (△); and Grasley and Lange (44), w/c = 0.4 (◁), w/c = 0.5 (▷). (*B*) Thermal expansion coefficient according to NRB theory, compared to tests of Meyers (45) (◇); Mitchell (46) (□); Dettling (47) (○); and Grasley and Lange (44), w/c = 0.4 (+), w/c = 0.5 (×).

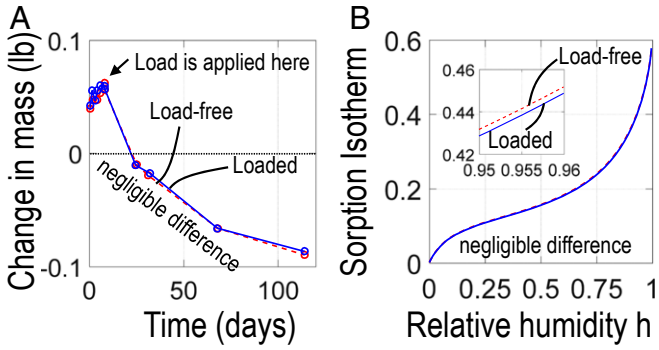

Fig. 5. (*A* and *B*) Drying tests (*A*) (48) demonstrating negligible water loss caused by applied uniaxial compression $0.5f_c'$ and (*B*) confirmed here by calculations.

dilatation at $h = 0.5$ is captured. The discrepancy seen at lower h in Fig. 4*B* might not be by chance and may require model refinement.

7. Load Effect on Water Content. The consolidations theory of concrete creep was discredited by Hansen's (48) tests which showed that prisms under uniaxial compression lose moisture by drying at about the same rate as load-free specimens. The change of each pore size caused by the load can be approximately considered as proportional to the change of porosity,

$$\frac{\Delta w}{w} = \frac{\Delta\zeta}{\varphi_0}, \text{ and } \frac{\mathrm{d}\beta}{\mathrm{d}w}(w + \Delta w) = \frac{\mathrm{d}\beta}{\mathrm{d}w}(w) + \frac{\mathrm{d}^2\beta}{\mathrm{d}w^2}(w)\Delta w, \quad \textbf{[21]}$$

where $\Delta\zeta$ is given by Eqs. **16** and **17** under the drained condition and $\mathrm{d}\beta(w)/\mathrm{d}w$ by Eqs. **1** and **3**. The shifted β function for the pore size distribution formulated here, along with Eq. **2**, can be used to compute the sorption isotherm shown in Fig. 5 (with the fitting parameters $c_T = 7.2$, $q = 2.07$, $\bar{q} = 2.57$; $w/c = 0.52$). Fig. 5 shows that the load-induced change of water content at constant humidity is less than the typical test error, which agrees with Hansen's finding.

Comments on Some Implications and Ramifications

Fig. 2 hints at several effects of increasing the w/c of concrete mix: 1) The capillary water portion increases, and thus the difference of q and $\bar{q}$ gets bigger, which matches the empirical law found in ref. 49; 2) for $h \to 1$, the sorption isotherm slope increases, making q smaller; 3) the pores widen and the portion of wider pores computed from Eq. **3** grows, which leads to a lower equivalent pressure; and 4) the (total) porosity is greater (and so is b). For low w/c, despite a higher equivalent pressure, the total shrinkage is lower, because of a lower Biot coefficient. However, the higher pore pressure tends to increase creep, which may cause excessive long-time deformations with cracking and thus compromise the durability of structures. Note also that the internal surface areas of hydrated cement ($A_0 = \varphi_0/(2\theta(h)\delta_1)$ for $h = 1$), predicted here by on the basis of the NRB isotherm, are 232 and 255 $\mathrm{m}^2/\mathrm{cm}^3$ for Fig. 2 *A* and *B*. These values are in the proper range estimated in ref. 50, but are grossly overestimated by the BET isotherm.

The results in Fig. 3 reflect the recent conclusion that cement hydration per se is always expansive (19, 31). While the core undergoes autogenous shrinkage, the wetting front, spreading from the exposed surface, speeds up hydration, which causes swelling. For thick specimens (or large volume–surface ratios), the part that undergoes swelling plays at lower ages a lesser role, causing the self-desiccation with autogenous shrinkage to

dominate. The opposite happens for thin specimens, in which the swelling dominates virtually from the start and the expansion due to hydration continues indefinitely.

The temperature and moisture analysis can, fortunately, be decoupled because the ratio of the respective diffusivities is about 1,000:1. Thus, in typical thin specimens, the temperature increase can be considered uniform and the water content constant, causing the increase of h to be given directly by the sorption isotherm. Interesting is a comparison with the Guggenheim–Anderson–de Boer (GAB) theory (51), a widely used empirical generalization of BET isotherm intended to reduce the unrealistic steep rise of BET toward ∞ at $h \to 1$; see Fig. 4*A* and note that the parameters of these two curves must conform to approximately the same sorption isotherm (8). The reason is that the use of a modified $k(T)$ will shift the saturation humidity near $h = 1$ to a larger value and thus cause a change of mass. This also reaffirms the physical justification of the geometrical restriction in ref. 8 on the total volume of adsorption layers due to reduction by β_n of their vapor-exposed area.

Closing Comment. Our entire model rests on one and the same statistically derived isotherm—the NRB.

ACKNOWLEDGMENTS. Some preliminary research was supported under US Department of Energy, Nuclear Energy University Program Grant DE-AC07-05/D1457. Thanks for valuable comments are due to Prof. Matthieu Vandamme of Université Paris-Est.

1. E. Detournay, A. H.-D. Cheng, "Fundamentals of poroelasticity" in *Analysis and Design Methods*, C. Fairhurst, Ed. (Elsevier, 1993), pp. 113–171.
2. M. A. Biot, General theory of three-dimensional consolidation. *J. Appl. Phys.* **12**, 155–164 (1941).
3. O. Coussy, *Poromechanics* (John Wiley & Sons, 2004).
4. O. Coussy, *Mechanics and Physics of Porous Solids* (John Wiley & Sons, 2011).
5. M. Rubenstein, "Emissions from the cement industry" in *The Global Network for Climate Solutions (GNCS FACTSHEETS)*, A. Halliday, Ed. (The Earth Institute, Columbia University, 2012).
6. R. M. Andrew, Global CO_2 emissions from cement production. *Earth Syst. Sci. Data* **10**, 195–217 (2018).
7. E. Tajuelo Rodriguez *et al.*, Composition, silicate anion structure and morphology of calcium silicate hydrates (csh) synthesised by silica-lime reaction and by controlled hydration of tricalcium silicate (c3s). *Adv. Appl. Ceram.* **114**, 362–371 (2015).
8. H. T. Nguyen, S. Rahimi-Aghdam, Z. P. Bažant, Sorption isotherm restricted by multilayer hindered adsorption and its relation to nanopore size distribution. *J. Mech. Phys. Solids* **127**, 111–124 (2019).
9. Z. P. Bazant, H. T. Nguyen, Direct multilayer adsorption of vapor in solids with multiscale porosity and hindered adsorbed layers in nanopores. arXiv:1812.11235 (28 December 2018).
10. S. Brunauer, P. H. Emmett, E. Teller, Adsorption of gases in multimolecular layers. *J. Am. Chem. Soc.* **60**, 309–319 (1938).
11. E. P. Barrett, L. G. Joyner, P. P. Halenda, The determination of pore volume and area distributions in porous substances. I. Computations from nitrogen isotherms. *J. Am. Chem. Soc.* **73**, 373–380 (1951).
12. Z. P. Bažant, Thermodynamics of interacting continua with surfaces and creep analysis of concrete structures. *Nucl. Eng. Des.* **20**, 477–505 (1972).
13. Z. P. Bažant, M. Jirásek, *Creep and Hygrothermal Effects in Concrete Structures* (Springer, 2018), vol. 225.
14. K. Maekawa, T. Ishida, T. Kishi, *Multi-Scale Modeling of Structural Concrete* (CRC Press, 2008).
15. G. Best, A. Cross, M. M. Pintar, R. Blinc, Distribution of pore sizes in white cement paste from proton NMR spin-lattice relaxation. *Adv. Cem. Res.* **8**, 163–166 (1996).
16. Q. Huang, Z. Jiang, X. Gu, W. Zhang, B. Guo, Numerical simulation of moisture transport in concrete based on a pore size distribution model. *Cement Concr. Res.* **67**, 31–43 (2015).
17. P. A. Bonnaud, Q. Ji, B. Coasne, R. J.-M. Pellenq, K. J. Van Vliet, Thermodynamics of water confined in porous calcium-silicate-hydrates. *Langmuir* **28**, 11422–11432 (2012).
18. O. Coussy, Revisiting the constitutive equations of unsaturated porous solids using a Lagrangian saturation concept. *Int. J. Numer. Anal. Methods Geomech.* **31**, 1675–1694 (2007).
19. S. Rahimi-Aghdam, E. Masoero, M. Rasoolinejad, Z. P. Bažant, Century-long expansion of hydrating cement counteracting concrete shrinkage due to humidity drop from selfdesiccation or external drying. *Mater. Struct.* **52**, 11 (2019).
20. R. Badmann, N. Stockhausen, M. J. Setzer, The statistical thickness and the chemical potential of adsorbed water films. *J. Colloid Interface Sci.* **82**, 534–542 (1981).
21. Z. P. Bažant, A. B. Hauggaard, S. Baweja, F.-J. Ulm, Microprestress-solidification theory for concrete creep. I: Aging and drying effects. *J. Eng. Mech.* **123**, 1188–1194 (1997).
22. S. Rahimi-Aghdam, Z. P. Bažant, G. Cusatis, Extended microprestress-solidification theory for long-term creep with diffusion size effect in concrete at variable environment. *J. Eng. Mech.* **145**, 04018131 (2018).
23. R. Sinko, Z. P. Bažant, S. Keten, A nanoscale perspective on the effects of transverse microprestress on drying creep of nanoporous solids. *Proc. R. Soc. A Math. Phys. Eng. Sci.* **474**, 20170570 (2018).
24. T. C. Powers, T. L. Brownyard, The thermodynamics of adsorption of water on hardened cement paste. *J. ACI* **18**, 549–602 (1947).
25. O. M. Jensen, P. F. Hansen, Influence of temperature on autogenous deformation and relative humidity change in hardening cement paste. *Cem. Concr. Res.* **29**, 567–575 (1999).
26. M. Wyrzykowski, P. Lura, Effect of relative humidity decrease due to self-desiccation on the hydration kinetics of cement. *Cem. Concr. Res.* **85**, 75–81 (2016).
27. S. Rahimi-Aghdam, Z. P. Bažant, M. J. A. Qomi, Cement hydration from hours to centuries controlled by diffusion through barrier shells of CSH. *J. Mech. Phys. Solids* **99**, 211–224 (2017).
28. K. Kovler, O. M. Jensen, *Report 41: Internal Curing of Concrete-State-of-the-Art Report of RILEM Technical Committee 196-ICC* (RILEM Publications SARL, Bagneux, France, 2007), vol. 41.
29. S. Rahimi-Aghdam, M. Rasoolinejad, Z. P. Bažant, Moisture diffusion in unsaturated self-desiccating concrete with humidity-dependent permeability and nonlinear sorption isotherm. *J. Eng. Mech.* **145**, 04019032 (2019).
30. J. J. Brooks, P. J. Wainwright, Properties of ultra-high-strength concrete containing a superplasticizer. *Mag. Concr. Res.* **35**, 205–213 (1983).
31. Z. P. Bažant, A. Donmez, E. Masoero, S. R. Aghdam, "Interaction of concrete creep, shrinkage and swelling with water, hydration, and damage: Nano-macro-chemo" in *CONCREEP* (2015), vol. 10, pp. 1–12.
32. R. A. Helmuth, D. H. Turk, "Elastic moduli of hardened Portland cement and tricalcium silicate pastes: Effect of porosity" (Tech. Rep. 210, Portland Cement Association, Skokie, IL, 1966).
33. J. Kováčik, Correlation between Young's modulus and porosity in porous materials. *J. Mater. Sci. Lett.* **18**, 1007–1010 (1999).
34. F.-J. Ulm, G. Constantinides, F. H. Heukamp, Is concrete a poromechanics materials?—A multiscale investigation of poroelastic properties. *Mater. Struct.* **37**, 43–58 (2004).
35. V. Baroghel-Bouny, M. Mainguy, T. Lassabatere, O. Coussy, Characterization and identification of equilibrium and transfer moisture properties for ordinary and high-performance cementitious materials. *Cem. Concr. Res.* **29**, 1225–1238 (1999).
36. S. Sabri, J. M. Illston, "Isothermal drying shrinkage and wetting swelling of hardened cement paste" in *Fundamental Research on Creep and Shrinkage of Concrete*, F. H. Wittmann, Ed. (Springer, 1982), pp. 63–72.
37. V. Baroghel-Bouny, P. Mounanga, A. Khelidj, A. Loukili, N. Rafai, Autogenous deformations of cement pastes: Part II. W/c effects, micro–macro correlations, and threshold values. *Cem. Concr. Res.* **36**, 123–136 (2006).
38. Z. Jiang, Z. Sun, P. Wang, Internal relative humidity distribution in high-performance cement paste due to moisture diffusion and self-desiccation. *Cem. Concr. Res.* **36**, 320–325 (2006).
39. M. Abuhaikal, K. Ioannidou, T. Petersen, R. J.-M. Pellenq, F.-J. Ulm, Le Châtelier's conjecture: Measurement of colloidal eigenstresses in chemically reactive materials. *J. Mech. Phys. Solids* **112**, 334–344 (2018).
40. S. Miyazawa, P. J. M. Monteiro, Volume change of high-strength concrete in moist conditions. *Cem. Concr. Res.* **26**, 567–572 (1996).
41. L.-O. Nilsson, "Temperature effects in relative humidity measurements on concrete-some preliminary studies" in *Nordic Symposium on Building Physics* (Lund University, Lund, Sweden, 1987).
42. B. Persson, "Self-desiccation and chloride migration" in *Self-Desiccation and Its Importance in Concrete Technology: Proceedings of the Third International Research Seminar*, B. Persson, G. Fagerlund, Eds. (Lund University, Lund, Sweden, 2002), pp. 175–194.
43. F. Radjy, E. J. Sellevold, K. K. Hansen, "Isoteric vapor pressure: Temperature data for water sorption in hardened cement paste: Enthalpy, entropy and sorption isotherms at different temperatures" (Tech. Rep. Byg Rapport RR-057, Technical University of Denmark, Lyngby, Denmark, 2003).
44. Z. C. Grasley, D. A. Lange, Thermal dilation and internal relative humidity of hardened cement paste. *Mater. Struct.* **40**, 311–317 (2007).
45. S. L. Meyers, "Thermal expansion characteristics of hardened cement paste and of concrete" in *Proceedings of the Thirtieth Annual Meeting of the Highway Research Board* (Highway Research Board, 1951), vol. 30, pp. 193–203.
46. L. J. Mitchell, "Thermal expansion tests on aggregates, neat cements, and concretes" in *Proceedings - American Society for Testing and Materials* (American Society Testing Materials, W. Conshohocken, PA, 1953), vol. 53, pp. 963–977.
47. H. Dettling, *Die Wärmedehnung des Zementsteines, der Gesteine und der Betone* (Technische Hochschule, Otto-Graf-Inst., 1962).
48. T. C. Hansen, "Creep and stress relaxation of concrete: A theoretical and experimental investigation" in *Svenska Forskningsinstitutet För Cement Och Betong Vid Kungl* (Tekniska Högskolan, 1960).
49. Y. Xi, Z. P. Bažant, H. M. Jennings, Moisture diffusion in cementitious materials adsorption isotherms. *Adv. Cem. Base Mater.* **1**, 248–257 (1994).
50. J. J. Thomas, H. M. Jennings, A. J. Allen, The surface area of hardened cement paste as measured by various techniques. *Concr. Sci. Eng.* **1**, 45–64 (1999).
51. S. Brunauer, I. Odler, M. Yudenfreund, The new model of hardened Portland cement paste. *Highw. Res. Rec.* **328**, 89–107 (1970).